

Confinement within the use of Minkowski integral representation

V. Šauli¹

¹*Department of Theoretical Physics, NPI Rez near Prague, Czech Academy of Sciences*

Confinement defined as the absence of certain (colored in QCD) particle like excitations in S-matrix is investigated in the nonperturbative framework of Schwinger-Dyson equations solved in Minkowski space. We revise the method based on utilization of generalized spectral representation and improve existing techniques, such that the method turns to be particularly suited for strong coupling quantum field theories with confinement. The method is applied to strong quenched QED and to $SU(3)$ Yang-Mills theory in 3+1 dimensions. Result for the gluonic spectral function has been obtained, for which purpose the equation for the gluon propagator has been solved in the gauge invariant manner. The gluon propagator, instead of having a real pole, has an unusual infrared structure that consists from two oppositely signed Cauchy resonances.

PACS numbers:

I. INTRODUCTION

Confinement and chiral symmetry breaking are essential features of QCD, they govern the low energy processes as well as they dominate late hadronization phase of high energy collisions. The confinement is phenomena that we do not observe the excitations of quark and gluon fields as a particle in isolation, while the chiral symmetry phenomena is associated with explanation of mass hierarchy of hadrons. These phenomena are intuitively well understood, however they are not yet satisfactorily encoded in a known framework which might be useful for calculations of hadronic observable e.g. continuous production form factors. Presented paper is devoted to the first unavoidable step: to the accurate evaluation of Green's function in strongly coupled QFT in the entire region of momentum Minkowski space.

QCD is gauge quantum field theory and therefore it requires a particular gauge fixing to be manageable in practice. Owing to a given gauge a particular confinement pictures have emerged in various studies. The Gribov-Zwanziger picture of confinement [1],[2] is likely established in Coulomb gauge [3], while not confirmed in the class of linear gauges (e.g. in Landau gauge), where the lattice simulation of ghost propagator does not show enhancement- the required condition for the Gribov-Zwanziger scenario. Other scenario of confinement- the vortex condensation [4–9] with associated condensation of magnetic monopoles are detected on lattices in special gauges [10],[11],[12], e.g. in maximal Abelian gauge [13]. Thus a different manifestation and realizations of confinement exist in various gauges, while they do not show up in other gauges. Actually, reflecting the difficulty of calculation performance, an overwhelming majority of canonical Schwinger-Dyson equations (SDEs) studies exist in the Landau gauge- a single example ($\xi = 0$) out of a larger class of linear gauges $\xi \neq 0$.

Provided the structure of Green's functions is known in the entire region of Minkowski space, the analytical properties of correlator associated with confined modes could clarify the topic of confinement in a great extent. Following the intuition one can expect that the correlator, which does not show up any peak or cusp in the spectrum can be ascribed to confined objects. While those peaks associated with particle like excitations and which stay pronounced in the S-matrix, they belong to standard observable particle excitations: freely moving particles or familiar hadronic resonances.

What might be an expected structure of confining modes is largely speculated in waste amount of literature and here we concern only those, that does not contradict standard analyticity and Unitarity. In case of QCD, the spectral decomposition or integral representation methods follow such a strategy [14–16]. The spectral decomposition of the Landau gauge lattice propagators have been questioned in papers [17, 18]. The resulting spectral function of lattice gluon propagator was found to be a smooth function and the absence of the real pole in the propagator can be taken as a striking evidence of confinement.

In order to shed a more light on this subject, we are going to concern several correlators and ask what is the relevant "spectral" structure of associated presumably confined objects in given approximation. To achieve desired analytical properties (i.e. spectrality) we develop relatively powerful technique, which rely on two steps analytical continuation of DSEs in between Minkowski and Euclidean space. The first step requires converting the SDEs system in momentum space into the equation for spectral functions by method analytical continuation. Although this is very conventional and certainly not new step when solving SDEs, [14–16, 19–24] it, up to the exception, did not provide convergent system of equations for strongly coupled theories with confinement. To achieve the later, we follow the trick introduced in [15] and perform the finite subtraction at the timelike scale of the momentum and perform the search of the solution, which is consistent with the spectrality constrain. It not only works, but it automatically ensures that obtained solution must be equivalent to the solution of the Euclidean space counterpart DSE.

In the next Sections II we explain how to get spectral function within the simple model: the quenched QED in 3+1 dimensions. Using the L renormalization scheme [25] we also marry the phenomena of mass generation and confinement with spectral representation of the electron propagator in classically massless case $m = 0$, keeping all renormalization constant finite and equal to one.

The method is also applied to the Background Field Method- Pinch Technique (BFM-PT) DSE in Landau gauge, which equation has been already studied in the paper [16] with limited numerical outputs. In the Section IV we revise numeric used in [16] and offer much precise solution there.

II. STRONG QUENCHED QED IN 3+1 DIMENSIONS

Strong coupling QED3+1 represents the truncation of DSEs system where the technique and associated amount of calculations is reduced to minimum. For classically massless fermions it requires the introduction of scale by hand. Using a hard cut-off it, the model was already studied in seventies [26], where the absence of the fermion pole was noticed due to the obscure grow of the electron dynamical mass function at large timelike q^2 . Notably, the model can be interpreted as an extreme case of the so called Walking Technicolor theory, where cut-off plays the role of the scale where asymptotic freedom start to emerge.

In the chiral limit, the classical Lagrangian mass is taken zero $m = 0$ and if a nontrivial mass function is generated, we use to use say it is generated dynamically through quantum loops. Such effect is most easily studied within the use of Euclidean metric, whilst to gain further information about confinement property of generated modes is less straightforward. The known critical behavior associated with Miransky scaling $M(0) \simeq \Lambda \exp(\alpha - \pi/3)^{-1/2}$ persists in more sophisticated approximations [28] and is associated with chiral symmetry breaking- generation of the mass. However even in classically massive case, the system can be characterized by the critical coupling $\alpha_c \simeq \pi/3$. For couplings satisfying inequality $\alpha < \alpha_c$ one gets non-confining spectral solution for the fermion propagator [22]. Such spectral function has a delta function associated with free propagation delta function plus the continuum part, which start to be nonzero at the threshold (identical to pole mass). We argue such solution does not exist for super-critical couplings $\alpha > \alpha_c$, for which case we provide another -confining- spectral solution for the first time. Avoiding hard cutoff is a net but necessary change which is required in our study, albeit in a very strict sense we are facing different theories since regularization plays it own role in quenched QED. For regularization we need to use more sophisticated regularization/renormalization scheme such us dimensional regularization [29], BPHZ scheme [30] or an L-operation scheme [25], which introduce the mass scale in a slightly different manner.

Conventional renormalization schemes (dimensional or BPHZ one, to name some out of the above list) together with simultaneous use of the spectral representation for the fermion propagator S :

$$S(k) = \int_0^\infty da \frac{\not{p}\rho_v(a) + \rho_s(a)}{p^2 - a + i\epsilon} \quad (2.1)$$

always forces us to renormalize the mass. The reason is that the Euclidean space loop integral turns to be divergent, irrespective of absence or presence of mass term in the Lagrangian. Thus to cover $m = 0$ case, we adopt L- regularization scheme, which does not require subtraction and allows to match spectral representation with dynamical mass generation in the chiral limit.

Our convention for Minkowski metric tensor reads: $g_{\mu\nu} = \text{diag}(+1, -1, -1, -1)$. Minkowski momenta are not labeled in our notation, while we write indices E when we want to specify the Euclidean momentum, i.e. for instance $q_E^2 = -q^2$ for some spacelike momentum q .

The unrenormalized quenched ladder-rainbow approximated fermion DSE in the Landau gauge reads:

$$\begin{aligned} S^{-1} &= \not{p} - m_o - \Sigma(p) \\ \Sigma(p) &= ie^2 \int \frac{d^4k}{(2\pi)^4} \gamma^\mu S(k) \gamma^\nu \frac{P_{\mu\nu}(k-p)}{(k-p)^2 + i\epsilon}, \end{aligned} \quad (2.2)$$

where e is the fermion charge, $P(z)$ is transverse projector. Two functions or distributions $\rho_{v,s}$ in the Eq. (2.1) are enough to complete two scalar functions $S_{v,s}$ or A, B alternatively. In our notation the are defined as

$$S(p) = S_v(p) \not{p} + S_s(p) = \frac{1}{\not{p}A(p^2) - B(p^2)}. \quad (2.3)$$

Dimensional renormalization scheme

Substituting the representation (2.1) into the DSE, swapping the order of integrations and making the integration over the momentum one gets

$$\begin{aligned} B(p^2) &= m_0 + \frac{3e^2}{(4\pi)^2} \int_0^\infty da \rho_s(a) \int_0^1 dt \left(\ln \left[\frac{p^2 t - a + i\epsilon}{\mu_t^2} \right] + C \right) \\ &= m(\mu_t) + \frac{3e^2}{(4\pi)^2} \int_0^\infty da \rho_s(a) \int_0^1 dt \ln \left[\frac{p^2 t - a + i\epsilon}{\mu_t^2} \right], \\ A &= 1 \end{aligned} \tag{2.4}$$

where μ_t is t'Hooft renormalization scale of MS bare dimensional renormalization scheme, which has been used.

In the next step we will add the zero of the following form

$$0 = B(\zeta) - m(\mu_t) - \frac{3e^2}{(4\pi)^2} \int_0^\infty da \rho_s(a) \int_0^1 dt \ln \left[\frac{\zeta t - a + i\epsilon}{\mu_t} \right] \tag{2.5}$$

to the rhs. of (2.4), i.e. we subtratct the equation with itself evaluated at the scale ζ . We thus get

$$B(p^2) = B(\zeta) + \frac{3e^2}{(4\pi)^2} \int_0^\infty da \rho_s(a) \int_0^1 dt \ln \left[\frac{p^2 t - a + i\epsilon}{\zeta t - a + i\epsilon} \right]. \tag{2.6}$$

Note also, the function $M = B/A$ is renormalization scheme invariant here as well as in other gauges.

DSE in L- renormalization scheme

The momentum integral stays divergent in dimensional regularization prescription and the singular pole term $1/\epsilon_d = 1/(d-4)$ in the constant C is absorbed into the renormalized mass, such that

$$m(\mu_t) = m_0 - \frac{3e^2}{(4\pi)^2} \int_0^1 da \rho_s(a) [1/\epsilon_d + \gamma_E + 4\pi] \tag{2.7}$$

In order to maintain renormalizability, mass term is inevitably presented, otherwise spectral representation could not be used in this scheme.

Recall, the derivation of the equation (2.4) is crucially based on the change of ordering of the several integrations. In order to include $m_0 = 0$ case as well, one unavoidably needs to keep the trace of selfenergy finite. For this purpose it is more convenient to use regularization called L - operation ([25]), which is based on further exploitation of Feynman parameterization, which does not require subtraction of infinities at least at one loop level. Applying this in our case, we get

$$\begin{aligned} B(p^2) &= m_0 + \frac{3e^2}{(4\pi)^2} \int_0^\infty da \rho_s(a) \int_0^1 dt \ln \left[\frac{p^2 t - a + i\epsilon}{\mu_F^2} \right], \\ A &= 1, \end{aligned} \tag{2.8}$$

The second term on the right side represents regularized self-energy in L operation scheme and since the expression is finite, the main outcomes is that to take $m_0 = 0$ is formally possible.

Subtracting the Eq. (2.8) at some timelike scale ζ , we get the Eq. (2.6) again. In this tricky way, we are able to include massless case as well, however stress here, that what make difference between dynamical mass generation in classically massless and in classically massive theory, is the property of solution. In our case, that the solution of (2.6) should provide the solution of Eq. (2.8) as well. It also means there must exist unique parameter μ_F , which complies with the existence of assumed spectral representation (2.1) in case of chiral limit.

Since the quenched QED in 3+1D is not an asymptotically free theory, there are other subtleties. Thus a hard cutoff was introduced in order to regularize momentum space integral in the Euclidean space theory [26]. It makes nonperturbative solutions obtained within the spectral technique herein, very hardly comparable with the Euclidean solution in details. Quenched LRA QED in 3+1 dimensions split into different models according to what regularization method is used. Let us anticipate at this place, that we do not see meaningful numerical solution in the chiral limit in quenched QED. All observed solutions are in fact indistinguishable from the explicitly massive case. However, as known from QCD studies, we expect that the entire dynamically mass generation can be studied within proposed method in asymptotically free theories.

The method of solution

For the spacelike p^2 and the negative ζ we can in principle drop out Feynman $i\epsilon$ and solve the equation in the spacelike domain of Minkowski space. Note plainly, that for this purpose one should know the spectral function ρ_s in advance. There is no working method (at least known to the author), which would allow to extract spectral function $\rho_{v,s}$ by solving DSE in the spacelike region alone. However it turns that the Eq. (2.6) is quite easily solvable numerically.

In order to determine the function ρ it is advantageous to consider the Eq. (2.4) at timelike scale, where the running mass B is complex valued function. The analytical continuation of the DSE (2.6) for $p^2 > 0$ can be written as

$$\begin{aligned}\Re B(p^2) &= \Re B(\zeta) + \frac{3e^2}{(4\pi)^2} \int_0^\infty da \rho_s(a) \int_0^1 dt \ln \left| \frac{p^2 t - a}{\zeta t - a} \right|, \\ \Im B(p^2) &= -\frac{3e^2}{16\pi} \int_0^\infty da \rho_s(a) \left[\left(1 - \frac{a}{p^2}\right) \theta(p^2 - a) - \left(1 - \frac{a}{\zeta}\right) \theta(\zeta - a) \right],\end{aligned}\quad (2.9)$$

with $\theta(x)$ is usual Heaviside step function, which for $x > 0$ $\theta(x) = 1$ and $\theta(x)$ is zero otherwise.

Keeping the equation for the dynamical mass function B in hand, one can reconstruct the propagator S . Comparing the real and the imaginary parts of the Eq. (2.6) and the Eq.(2.1) one can write down the following complementary equation:

$$\rho_s(s) = \frac{-1}{\pi} \frac{\Im B(s) R_D(s) + \Re B(s) I_D(s)}{R_D^2(s) + I_D^2(s)} \quad (2.10)$$

where $s = p^2 > 0$ in our metric, and where the functions R_D and I_D stand for the square of the real and the imaginary part of the function $sA^2(s) - B^2(s)$, i.e.

$$\begin{aligned}R_D(s) &= s[\Re A(s)]^2 - s[\Im A(s)]^2 - [\Re B(s)]^2 + [\Im B(s)]^2, \\ I_D(s) &= 2s\Re A(s)\Im A(s) + 2\Re B(s)\Im B(s),\end{aligned}\quad (2.11)$$

where we keep A non constant for more general purpose ($A = 1$ in the approximation employed here).

To get the solution, we start with some ad hoc initial guess for the constant $\Im B(\zeta)$ and trial spectral function $\rho_s(s)$ and substitute it into the Eq. (2.9). Then three equations (2.9) and (2.10) have been solved numerically by method of iterations. Very importantly, the method works equally well in case of QCD quark propagator [15, 23].

In this way the obtained function ρ_s is still not what we are looking for. The system is ill constrained by our random choice of the complex phase $\phi = \arg \Im B(\zeta) / \Re B(\zeta)$ and only thanks to high nonlinearity it provides precise numerical solution with the arbitrarily high numerical accuracy. Recall, there must exist a single value $\Im B(\zeta)$ for a fixed mass $\Re(\zeta)$ at fixed scale ζ . To get rid of the problem we fix $\Re B(\zeta)$ and repeat iteration procedure described above for a new value $\Im B(\zeta)$ and look at the quality of equality:

$$L(s) = R(s) = \frac{1}{4} \Re Tr S(s) = \Re S_s(s) \quad (2.12)$$

where

$$\begin{aligned}L(s) &= P. \int_0^\infty da \frac{\rho_s(a)}{p^2 - a} \\ R(s) &= \frac{-\Im B(s) I_D(s) + \Re B(s) R_D(s)}{R_D^2(s) + I_D^2(s)}\end{aligned}\quad (2.13)$$

for a given choice of the phase $\phi(\zeta)$. Similar constrains can be written for the function S_v (see Appendix), however in our approximation S_v is completely, albeit non-linearly, determined by the function S_s itself.

In the Fig. (1) solid line represents result for the propagator which corresponds to the ratio $\Im B(0.1) / \Re B(0.1) = 0.325 \pm 0.005$. The real part of $B(\zeta)$ is our choice, while the imaginary part $\Im B(\zeta = 1)$ was the subject of the numerical scan. In order to visualize our numerical search we plot two lines corresponding to L and R as defined in by (2.13). Lines are labeled by two numbers representing values $\Re B(\zeta), \Im B(\zeta)$. More they can be distinguished, more the equality Eq. (2.12) is incomplected.

The absence of the real pole in the propagator is more then obvious and instead of physical threshold the propagator has the zero branch point. The imaginary part of propagators for super-critical coupling does not correspond to the decay width of particle mode, but rather it tells us how much fast is the creation-reabsorption process of associated quantum field. Confinement is there due to the abrupt generation of absorptive part of selfenergy in infrared domain of the timelike momenta. It is worthwhile to mention that the generation of zero anomalous threshold is the old

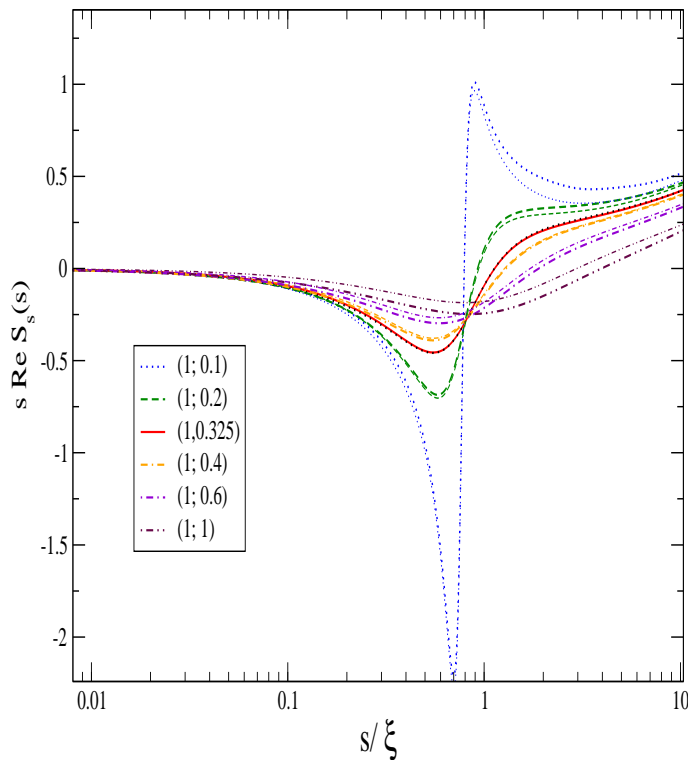


FIG. 1: $sS(s)$ function constructed from L and R functions. Each type of line corresponds to a given choice of the phase, they are labeled by real and imaginary part of $B(\zeta)/\zeta$. The exception is the best matching case, where “L” is dotted, while “R” solution is depicted by the solid line.

conjecture of Schwinger [27] made for 1+1 QED, which has emerged several years before QCD has been accepted as a correct theory of hadrons.

In the Fig. 2 we show the spectral function of the fermion propagator. In non-confining quantum field theory, the Osterwalder-Schrader axiom of reflection positivity [31] is equivalent to the positive definiteness of the norm in Hilbert space of the corresponding Quantum Field Theory. Violation of reflection positivity is often regarded as a manifestation of confinement. Obviously the property of reflection positivity is not lost in our case, however the fermion turns to be a short living excitation according to suggestion made (albeit for the photon at that time) by J. Schwinger half century ago. Violation of reflection positivity turns out to be a weak criterion for confinement in the model presented herein.

We do not show the evolution with the coupling however within decreasing coupling the shape gradually rises elbows and the on shell pole rises for subcritical value of couplings. For small couplings then one needs to determine the pole position and its residuum as done for theory in even dimensions [22],[21] as well as for theory with odd number of spacetime dimensions [32]. We also do not go beyond quenched approximation due to the Abelian character of the interaction, however we can expect that when the photon polarization function is taken into account, the quantitative changes can be quite dramatic.

At last but not at least, as we have already anticipated, we do not get any truly conformal solution. The renormalization scale makes the theory effectively massive and in order to eliminate scale μ_F completely one would need the condition $\int \rho(a) = 0$ is fulfilled. The later we have not achieved herein.

III. YANG-MILLS THEORY, CONFINEMENT OF GLUONS

The analytical structure of the gluon propagator on the entire domain of momenta is largely unknown. The ultraviolet behavior of the gluon propagator should be governed by perturbation theory, while at low q^2 it is partially known only at the spacelike domain of momenta, where it is accessible by lattice theory and other Euclidean space nonperturbative methods.

For our purpose we will use a simple truncation of the PT-BFM [33] gluon Dyson-Schwinger equation which has been already studied in [34, 35] in the Euclidean space and in the paper [16] in the Minkowski space. Remind that

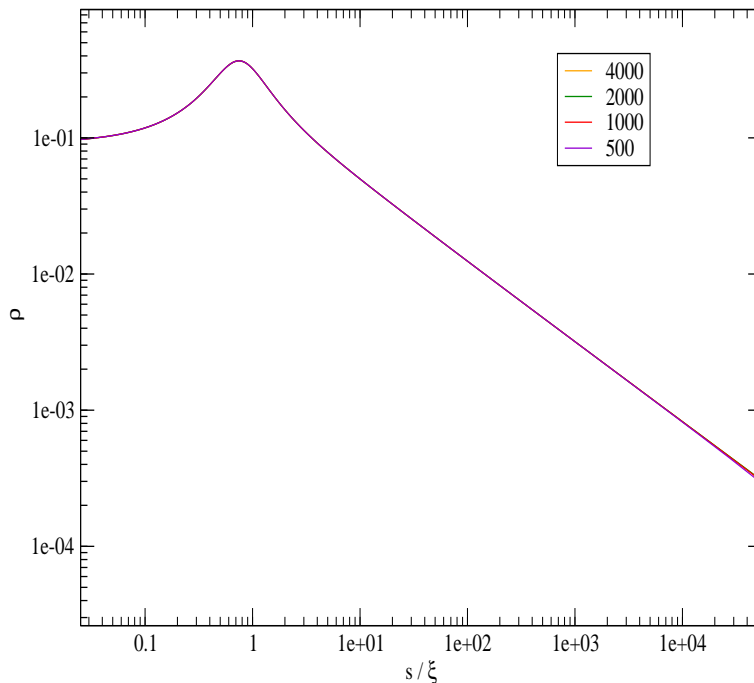


FIG. 2: Spectral function of strongly interacting fermion in units of renormalized mass ζ .

the Background Field method (BFM) fields and Pinch Technique (PT) are originally perturbative constructs in which Green's function satisfy Ward identities rather than Slavnov-Taylor identities. Guiding by the principles of Pinch Technique, the gauge invariant truncation of Yang-Mills DSEs was constructed, providing nonperturbative gauge invariant Green's functions (in any covariant gauge[36]). Apart of lattice development, there exists a certain progress [44, 46–50] in developments of SDEs in Yang-Mills theory in various gauges. However, since the most of studies are performed in Landau gauge we have chosen this gauge as well.

Here, using the method of subtractions in the timelike scale we revise numeric used in [16] and offer much precise solution. We show that instead of two sharp poles as naively suggested in [16], we get the solution characterized by a smooth spectral function with few nodes and several modes of opposite signs.

To get infrared finite gluon propagator, the gluon propagator must lose its perturbative $1/q^2$ pole through the Schwinger mechanism in Yang-Mills theory [51]. It underlies on the assumption of the form of transverse piece of the gluon vertex in a way it leaves polarization tensor gauge invariant (transverse to its momentum). In this paper we simply use the derived equation in [34], where Schwinger mechanism is employed through the simple Ansatz for the unproper (two leg dressed) three gluon PT-BFM dressed vertex

$$d(k)\tilde{\Gamma}_{\nu\alpha\beta}(k, q)d(k+q) = \int d\omega \rho(\omega) \frac{1}{k^2 - \omega + i\epsilon} \Gamma_{\nu\alpha\beta}^L \frac{1}{(k+q)^2 - \omega + i\epsilon} + d(k)\tilde{\Gamma}_{\nu\alpha\beta}^T d(k+q), \quad (3.1)$$

where $\Gamma_{\nu\alpha\beta}^L$ satisfies tree level WTI and d is scalar function related to the all order PT-BFM gluon propagator which in Landau gauge reads

$$G^{\mu\nu} = \left[-g^{\mu\nu} + \frac{k^\mu k^\nu}{k^2} \right] d(k^2) \quad (3.2)$$

and satisfies generalized Lehman representation

$$d(k^2) = \int_0^\infty d\omega \frac{\rho(\omega)}{k^2 - \omega + i\epsilon} \quad (3.3)$$

and $\tilde{\Gamma}_T$ is the rest of the three gluon unproper vertex which is not specified by gauge invariance. In the expression (3.3) we assume the branch point is located in the beginning of complex plane, albeit not generated by poles, it is in its usual “non-anomalous” position.

The essential feature of the vertex $\Gamma_{\nu\alpha\beta}$ is that apart the structure dictated by WTI it also includes $1/q^2$ pole term which gives rise to infrared finite solution. For this purpose the following form

$$d(k)\tilde{\Gamma}_T^{\nu\alpha\beta}(k, q)d(k+q) = \int d\omega\rho(\omega)\frac{1}{k^2-\omega+i\epsilon}\Gamma_{\nu\alpha\beta}^T\frac{1}{(k+q)^2-\omega+i\epsilon}$$

$$\Gamma_T^{\nu\alpha\beta}(k, q) = c_1[(2k+q)_\nu + \frac{q_\nu}{q^2}(-2k\cdot q - q^2)]g_{\alpha\beta} + [c_3 + \frac{c_2}{2q^2}((k+q)^2 + k^2)](q_\beta g_{\nu\alpha} - q_\alpha g_{\nu\beta}), \quad (3.4)$$

has been proposed in [34]. This vertex is transverse in respect to q ($q\cdot\Gamma = 0$) and it respects Bose symmetry to two quantum legs interchange.

After the renormalization, it leads to the following form of SDE in Euclidean space:

$$d_E^{-1}(q_E^2) = q_E^2 \left\{ K + bg^2 \int_0^{q_E^2/4} dz \sqrt{1 - \frac{4z}{q_E^2}} d_E(z) \right\}$$

$$+ \gamma bg^2 \int_0^{q_E^2/4} dz z \sqrt{1 - \frac{4z}{q_E^2}} d_E(z) + d_E^{-1}(0), \quad (3.5)$$

where the second line appears due to the Ansatz for the gluon vertex (3.4) and K is the renormalization constant. Thus the strength of the dynamical mass generation is triggered through the adopted coupling constants c_1, c_2, c_3 which is fully equivalent to the introduction of (in principle arbitrary) constant γ and infrared value $d_E^{-1}(0)$ (for completeness recall that in the paper [34] $d(0)$ has been calculated since one of c_i was fixed by hand).

Analytical continuation $q_E^2 = -q^2 = -s \rightarrow q^2, s = q^2 > 0$ of the Eq. (3.5) is very straightforward and the gap equation for the gluon propagator for timelike variable s reads

$$d^{-1}(s) = s \left\{ K + bg^2 \int_0^{s/4} dz \sqrt{1 - \frac{4z}{s}} d(z) \right\} + \gamma bg^2 \int_0^{s/4} dz z \sqrt{1 - \frac{4z}{s}} d(z) + d^{-1}(0) + i\epsilon \quad (3.6)$$

where we use standard convention $d_E(q_E^2) = -d(s)$ for $s = q^2 < 0$ and absorb the sign into the definition of Minkowski space gluon propagator. Note, the inverse propagator $d^{-1}(0)$ should take a negative value to prevent tachyonic solution.

Subtracting the equation once again at the timelike fixed scale ζ one gets:

$$d^{-1}(s) = s \left\{ K + bg^2 \int_0^{s/4} dz \sqrt{1 - \frac{4z}{s}} d(z) \right\} - (s \rightarrow \zeta)$$

$$+ \gamma bg^2 \int_0^{s/4} dz z \sqrt{1 - \frac{4z}{s}} d(z) - (s \rightarrow \zeta) - d^{-1}(\zeta). \quad (3.7)$$

Now, the function d is assumed to be complex for all $s > 0$, while it stays real for negative s .

Like in previous study of quenched QED, we should mention that the DSE equation (3.7) has infinity many stable solutions that do not match the Eq. (3.8) and the numerical scan of the phase of the function $d(\zeta)$ must be performed. Thus we arbitrarily fix the real part $\Re d^{-1}(\zeta)$ at some fixed scale ζ and then search for the value of $\Im d^{-1}(\zeta)$ till assumed integral representation, e.g. the relation

$$\Re d(k^2) = \frac{-1}{\pi} P. \int d\omega \frac{\Im d(\omega)}{k^2 - \omega}, \quad (3.8)$$

will hold.

Like in previous study of quenched QED, we should mention that the DSE equation (3.7) has infinity many stable solutions that do not match the Eq. (3.8) and the numerical scan of the phase of the function $d(\zeta)$ must be performed.

Recall, that while detailed values of renormalization constant K and $d^{-1}(0)$ are not crucial for the subject of confinement, they should match with other quantities calculated in given specific scheme [45]. Notably, the gluonic gap Eq. (3.5) is derivable in various symmetry preserving renormalization scheme, to name a few: BPHZ MOM scheme, the dimensional renormalization as well as it can be obtained within the L operational scheme [25]. All these schemes necessarily lead to the Eq. (3.7). Contrary to this, an unintegrated form of the Eq. (3.5) does not necessary ensure the same result when one uses regularization technique, which does not respect symmetry of the theory and fake unphysical solutions can appear.

The solution of the gluon propagator is shown in the figures 3 and 4, where only the solution fitting the Eq. (3.8) is shown. The shape of the gluon propagator at the timelike region is obviously something that we are not experienced, the real part is represented by two broad peaks which have simultaneously opposite signs.

To get presented solution we set $\Re\zeta d(\zeta) = 1.8570$ and couplings were chosen such that $g^2 = 15.5$, $\gamma = 1/20$. We got $\Im\zeta d(\zeta) = 0.140$ after the scan. Comparison of gluonic SDE with RGE improved SDE is shown as well (interested reader can find the meaning in [16]). Contrary to achievements in [16], now the access to numerical solution in the whole complex plain is an easy and straightforward and the reader can find our numerical codes at the author's web page.

At ultraviolet the studied gluon propagator vanishes as $1/(s \ln^\gamma)(s)$ with $\gamma \simeq 0.5$. This behavior should lead to superconvergent relation sum rule [37],[38],[39]:

$$I = \int_0^\infty \rho(s) ds = 0, \quad (3.9)$$

which turns to be satisfied within reasonable accuracy $I \simeq 0.05$.

A kind of the resonance with zero mass anomalous threshold of the form

$$\rho(s) = \frac{s\gamma}{(s^2 - s_o^2\kappa)^2 + (s\Gamma)^2} \quad (3.10)$$

was suggested as an artificial mathematical model for the spectral function of the photon in the Schwinger model [27]. Interestingly, the spectral gluon function can be quite accurately parametrized as a difference of two near short living excitations. Comparing to Schwinger model, there are unavoidable further but subtle changes since $SU(3)$ gluodynamics should comply with asymptotic freedom, e.g. with the spectral sum rule (3.9), thus instead of using (3.10), it turns that more suited fit can be constructed from the sum of several Cauchy distributions

$$\rho(s) = \sum_i [R \frac{(s/\zeta)^\lambda}{(s - s_o)^2 + (\Gamma)^2}]_i, \quad (3.11)$$

where the exponent $\lambda = 0$ for the positive modes of the function ρ (negative modes in figures), while for the negative mode the exponent $\lambda = 3/4$ was taken. Only two such contribution are basically enough to describe entirely gluon propagator in the infrared. Fitting the first peak structure at 800MeV (a typical value estimated by others), the second peak then appears at 1110 MeV. More precise numerical fit is presented in the Appendix B.

It is interesting to see how much the PT-BFM gluon propagator differs from the conventional gluon propagator. In the fig. 4 we also compare with fit of lattice data [40, 41]. Since the lattice gluon propagator is known at relatively small momentum region, the lattice data tolerate comparison to fits with drastically different analytical behavior. Actually, basically the same data complies with spectral fit [42], with fit with complex conjugated poles [40, 42] and much newly with on-shell single plus double pole fit [43] (at quite low Euclidean region of q^2). Since we are comparing two theoretically rather different objects, anyone of aforementioned lattice data fits is suited for purpose of our visual comparison. The differences are obviously large, quantitatively comparable to difference between gluon propagators calculated in the Feynman and the Landau gauge [44].

IV. SHORT REMARK ON THE QUARK PROPAGATOR

Following similar method described in the Sect. 2 the ladder-rainbow approximation (LRA) for the quark SDE has been already solved in the paper [15]. The obtained quark propagator has an anomalous threshold located at beginning of complex plane of momenta. Also the confinement manifest itself as missing real pole in the quark propagator. On the other hand a simple phenomenological kernel used in [15] did not follow from QCD directly, and it is also failing in detailed description of anomalous correction of electromagnetic form factors.

To this point, let us mention that the LRA within a naive use of the lattice Landau gauge gluon propagator does not have enough strength to provide correct amount of chiral symmetry breaking. It is thus very likely that the kernel of LRA must mimic also the contribution from neglected crossed boxes as well as there should be involved changes due to the quark-gluon vertex (effectively but purely presented in the LRA).

In our case the scale invariant quantity $sd(s)$ is several times suppressed when comparing to lattice Landau gauge gluon propagator. Not surprisingly the LRA does not provide a known slope of the quark dynamical mass function, neither it can provide correct pion observable. The best understanding of this inefficiency is obvious from the modern version of Goldberger-Treiman-like relation [52],[53], which reads

$$f_\pi \Gamma_A(0, k) = B(k) \quad (4.1)$$

where Γ_A is the leading piece of the pion's Bethe-Salpeter amplitude and B is the quark dynamical mass times the quark renormalization function.

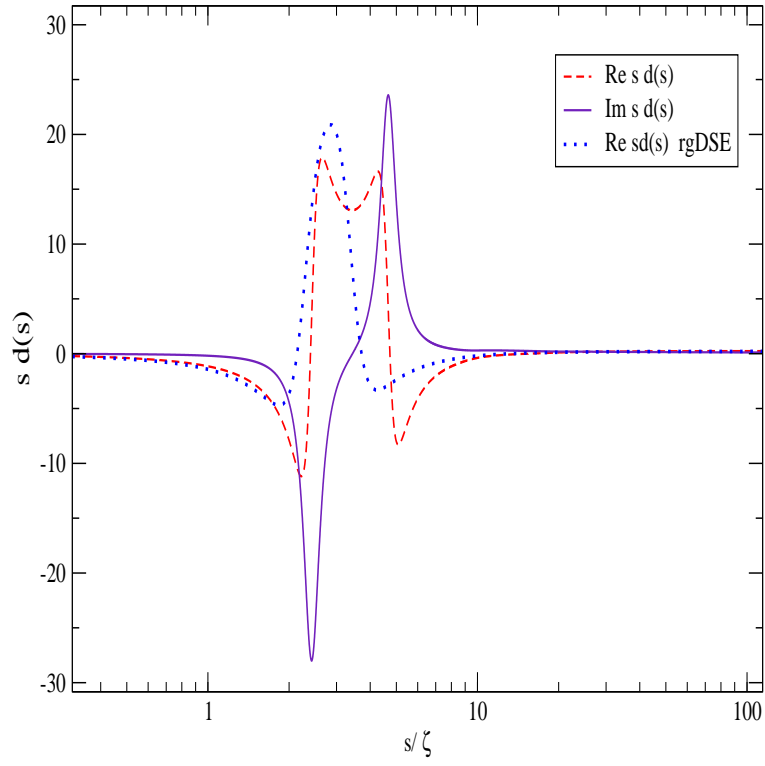


FIG. 3: DSE solution for the so-called solution for the so-called

the real part of the

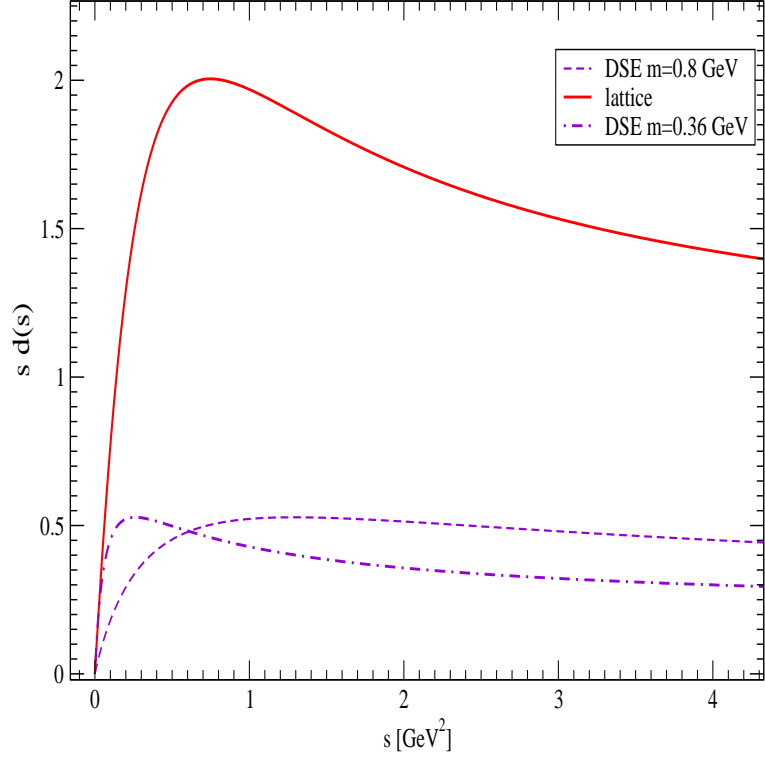


FIG. 4: Solutions of gluonic DSE compared to the lattice fit in the Landau gauge. Dot-dashed line states for rescaled solution which corresponds to 0.36 GeV position of the first peak in the gluon propagator.

To conclude: staying in Landau gauge then within the single gluon exchange approximation with gluon propagator calculated in BFM-PT scheme leads to the brutal underestimate of the total strength of the quark-antiquark scattering kernel. One needs to go beyond LRA in the Landau gauge at presented scheme, or as second tempting possibility, one can use the gauge where the LRA approximation is much appropriate when considering only the lowest skeleton graphs. Both possibilities and their mutual comparison deserve for future studies.

V. CONCLUSION

We have applied the method of subtractions of SDEs at the timelike scale of momenta and get the confined solution in Yang-Mills theory for the gluon propagator as well as we have illustrated the method in case of fermion propagator in quenched QED. In both strong coupling models the solutions for two point correlator were obtained in the entire domain of Minkowski space momenta. The method should be and in fact it has already been useful for evaluation of hadronic form factors.

Appendix A: Appendix A

The second constrains which should be checked beyond ladder-rainbow approximation can be derived by making the trace of \not{p} -projected fermion propagator, where

$$L_v(s) = R_v(s) = \frac{1}{4p^2} \Re \not{p} Tr S(s) = \Re S_v(s). \quad (\text{A1})$$

with the left and right hand sides defined as

$$\begin{aligned} L_v(s) &= P. \int_0^\infty da \frac{\rho_v(a)}{s-a} \\ R_v(s) &= \frac{-\Re A(s) R_D(s) + \Im A(s) I_D(s)}{R_D^2(s) + I_D^2(s)} \end{aligned} \quad (\text{A2})$$

where symbol $P.$ stands for principal value integration.

Appendix B: Appendix B

We provide the details of the numerical fit in this Appendix. The fit was chosen as following

$$\begin{aligned} \rho(s) &= \sum_{i=1,3} \frac{R_i}{(s - s_{o,i})^2 + (w_i)^2} \\ &+ \sum_{i=2,4} R_i \frac{(s/\zeta)^{3/4}}{(s - s_{o,i})^2 + (w_i)^2}, \end{aligned} \quad (\text{B1})$$

with the numerical values of parameters listed in the following table:

i	R/ζ	s_o/ζ	w/ζ
1	-0.465	2.4	0.2
2	0.25	4.63	0.39
3	-0.13	6.0	1.6
4	0.045	11.230	16.0

Proposed fit is compared to the obtained numerical results in the Fig. 5, note that the curve labeled as ‘‘Re fit’’ was obtained with the spectral function given by (B1) and used in the Eq. (3.3). The large ‘‘widths’’ as well as the small value of residuum of the fourth term makes this term already negligible.

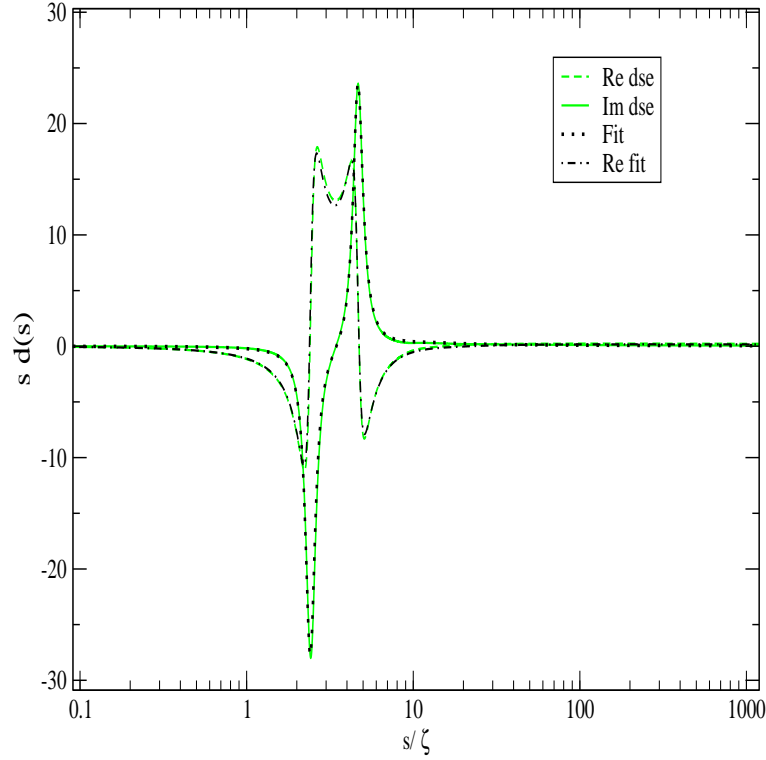


FIG. 5: Fit of the gluon propagator compared with the DSE numerical result.

- [2] D. Zwanziger, Nucl. Phys. B321, 591 (1989).
- [3] D. Epple, H. Reinhardt, W. Schleifenbaum, Phys. Rev. D75, 045011 (2007).
- [4] G. 't Hooft, Nucl. Phys. B138, 1 (1978).
- [5] P. Vinciarelli, Phys. Lett. 78B, 485 (1978).
- [6] T. Yoneya, Nucl. Phys. B144, 195 (1978).
- [7] J.M. Cornwall, Nucl. Phys. B157, 392 (1979).
- [8] G. Mack, V.B. Petkova, Annals Phys. 123, 442 (1979).
- [9] H.B. Nielsen, P. Olesen, Nucl. Phys. B160, 380 (1979).
- [10] L. Del Debbio, M. Faber, J. Greensite, S. Olejnik, Phys. Rev. D55, 2298 (1997).
- [11] K. Langfeld, H. Reinhardt, O. Tennert, Phys. Lett. B419, 317 (1998).
- [12] L. Del Debbio, M. Faber, J. Giedt, J. Greensite, S. Olejnik, Phys. Rev. D58, 094501 (1998).
- [13] J. D. Stack , W. W. Tucker, Roy J. Wensley, Nucl. Phys. B 639,203-222 (2002).
- [14] J.M. Cornwall, Phys. Rev. D26,1453 (1982).
- [15] V. Sauli, Few Body Syst. **61**, 3, 23 (2020).
- [16] V. Sauli, J. Phys. **G39**, 035003 (2012).
- [17] D. Dudal, O. Oliveira, and P. J. Silva, Phys. Rev. **D** 89 1, 014010 (2014).
- [18] R.-A. Tripolt, P. Gubler, M. Ulybyshev, L. Von Smekal, Comput. Phys. Commun. **237**, 129–142 (2019).
- [19] R. Delbourgo and P.C. West, J. Phys. A 10, 1049 (1977).
- [20] C. N. Parker, J. Phys. A, Math. Gen. 17, 2873 (1984).
- [21] V. Sauli, Few Body Syst. 61, 3, 23 (2020).
- [22] V. Sauli, JHEP 7(2), 1-36, (2003).
- [23] V. Sauli, Phys. Rev. **D** 102, 014049 (2020).
- [24] C. Mezraga and G. Salme, arXiv:2006.15947.
- [25] V. Sauli, arXiv:2009.07195.
- [26] R. Fukuda, T. Kugo, Nucl. Phys. **B** 117, 250 (1976).
- [27] J. Schwinger, Phys. Rev. **128**, 2425-2429 (1962).
- [28] A. Bashir, A. Raya, S. Sánchez-Madrigal, Phys. Rev. **D** 84, 036013 (2011).
- [29] Gerard 't Hooft, M.J.G. Veltman, Nucl. Phys. B 44,189-213 (1972).
- [30] N.N. Bogoliubov and O. S. Parasyuk, Dok. Akad. Nauk SSSR 100, 25–28 (1955).
- [31] K. Osterwalder and R. Schrader, Commun. Math. Phys **31**, 83 (1973). Cummun. Math. Phys. **42** , 281 (1975).
- [32] J. Horak, J. M. Pawlowski, N. Wink arXiv: 2006.09778.
- [33] D. Binosi, J. Papavassiliou, Phys. Rept. **479**, 1-152 (2009).

- [34] A.C. Aguilar, J. Papavassiliou, JHEP 0612:012, (2006).
- [35] J. M. Cornwall, Phys. Rev. **D80**, 096001 (2009).
- [36] A. Pilaftsis Nucl. Phys. **B** 487,467-491 (1997).
- [37] R. Oehme and W. Zimmermann, Phys. Rev. **D** 21, 471 (1980).
- [38] R. Oehme, Phys. Lett. **B** 252, 641–646 (1990).
- [39] J. M. Cornwall, Mod. Phys. Lett. **A** 28, 1330035 (2013).
- [40] D. Dudal, O. Oliveira, P. J. Silva, arXiv:1811.11678.
- [41] D. Dudal, O. Oliveira, M. Roelfs, P. Silva, Nucl. Phys. **B** 952, 114912 (2020).
- [42] A. G. Duarte, O. Oliveira, P. J. Silva, Phys. Rev. **D** 94, 014502 (2016).
- [43] S. W. Li, P. Lowdon, O. Oliveira, P. J. Silva, Phys. Lett. **B** 803 ,135329 (2020).
- [44] A. C. Aguilar, D. Binosi, J. Papavassiliou, Phys. Rev. **D** 91, 085014 (2015).
- [45] A. A. Natale, Braz. J. Phys. **37**, 306-312 (2007); arXiv:hep-ph/0610256 .
- [46] A. C. Aguilar, D. Binosi, J. Papavassiliou, Phys. Rev. **D** 88, 074010 (2013).
- [47] A. C. Aguilar, D. Binosi, C. T. Figueiredo, J. Papavassiliou, Phys. Rev. **D** 94, 045002 (2016).
- [48] A. C. Aguilar, D. Binosi, J. Papavassiliou, Phys. Rev. **D** 95, 034017 (2017).
- [49] A. C. Aguilar, M. N. Ferreira, C. T. Figueiredo, J. Papavassiliou, Phys. Rev. **D** 100, 094039 (2019).
- [50] C. S. Fischer, M. Q. Huber , arXiv:2007.11505.
- [51] A. C. Aguilar, D. Binosi, J. Papavassiliou, arXiv:1107.3968.
- [52] P. Maris, C. D. Roberts and P. C. Tandy, Phys. Lett. **B** 420, 267 (1998).
- [53] S.-X. Qin, C. D. Roberts and S. M. Schmidt, Phys. Lett. **B** 733, 202 (2014).